

Allogeneic Transplantation of Müller-Derived Retinal Ganglion Cells Improves Retinal Function in a Feline Model of Ganglion Cell Depletion

SILKE BECKER,^a KAREN EASTLAKE,^a HARI JAYARAM,^b MEGAN F. JONES,^a ROBERT A. BROWN,^c GILLIAN J. MCLELLAN,^d DAVID G. CHARTERIS,^b PENG T. KHAW,^b G. ASTRID LIMB^b

Key Words. Stem cells • Müller cells • Retinal ganglion cells • Retinal degeneration

^aInstitute of Ophthalmology,

^bNational Institute for Health Research Biomedical Research Centre for Ophthalmology, Institute of Ophthalmology, and

^cInstitute of Orthopaedics and Musculoskeletal Science, University College London, London, United Kingdom;

^dDepartment of Ophthalmology and Visual Sciences, University of Wisconsin School of Medicine and Public Health, Madison, Wisconsin, USA

Correspondence: G. Astrid Limb, Ph.D., F.R.C.Path., Division of Ocular Biology and Therapeutics, University College London Institute of Ophthalmology, 11-43 Bath Street, London EC1V 9EL, United Kingdom. Telephone: 20-7608-6974; E-Mail: g.limb@ucl.ac.uk

Received June 11, 2015; accepted for publication November 11, 2015; published Online First on December 30, 2015.

©AlphaMed Press
1066-5099/2015/\$20.00/0

[http://dx.doi.org/
10.5966/sctm.2015-0125](http://dx.doi.org/10.5966/sctm.2015-0125)

ABSTRACT

Human Müller glia with stem cell characteristics (hMGSCs) have been shown to improve retinal function upon transplantation into rat models of retinal ganglion cell (RGC) depletion. However, their translational potential may depend upon successful engraftment and improvement of retinal function in experimental models with anatomical and functional features resembling those of the human eye. We investigated the effect of allogeneic transplantation of feline Müller glia with the ability to differentiate into cells expressing RGC markers, following ablation of RGCs by *N*-methyl-D-aspartate (NMDA). Unlike previous observations in the rat, transplantation of hMGSC-derived RGCs into the feline vitreous formed aggregates and elicited a severe inflammatory response without improving visual function. In contrast, allogeneic transplantation of feline MGSC (fMGSC)-derived RGCs into the vitrectomized eye improved the scotopic threshold response (STR) of the electroretinogram (ERG). Despite causing functional improvement, the cells did not attach onto the retina and formed aggregates on peripheral vitreous remnants, suggesting that vitreous may constitute a barrier for cell attachment onto the retina. This was confirmed by observations that cellular scaffolds of compressed collagen and enriched preparations of fMGSC-derived RGCs facilitated cell attachment. Although cells did not migrate into the RGC layer or the optic nerve, they significantly improved the STR and the photopic negative response of the ERG, indicative of increased RGC function. These results suggest that MGSCs have a neuroprotective ability that promotes partial recovery of impaired RGC function and indicate that cell attachment onto the retina may be necessary for transplanted cells to confer neuroprotection to the retina. STEM CELLS TRANSLATIONAL MEDICINE 2016;5:192–205

SIGNIFICANCE

Müller glia with stem cell characteristics are present in the adult human retina, but they do not have regenerative ability. These cells, however, have potential for development of cell therapies to treat retinal disease. Using a feline model of retinal ganglion cell (RGC) depletion, cell grafting methods to improve RGC function have been developed. Using cellular scaffolds, allogeneic transplantation of Müller glia-derived RGC promoted cell attachment onto the retina and enhanced retinal function, as judged by improvement of the photopic negative and scotopic threshold responses of the electroretinogram. The results suggest that the improvement of RGC function observed may be ascribed to the neuroprotective ability of these cells and indicate that attachment of the transplanted cells onto the retina is required to promote effective neuroprotection.

INTRODUCTION

Glaucoma is a complex neurodegenerative condition characterized by progressive retinal ganglion cell (RGC) death and optic nerve degeneration [1, 2]. Current treatments aim to prevent disease progression by lowering intraocular pressure but do not restore lost visual function, for which development of cell-based therapies would potentially benefit patients affected by severe disease. Cell therapies could be potentially aimed at replacing damaged RGCs

or providing neurotrophic support to maintain the viability and function of remaining neurons. Müller glia with stem cell characteristics (MGSCs), which were first characterized in the zebrafish [3], have been identified in several mammalian species, including humans [4, 5]. We have previously shown that upon downregulation of Notch, a transcription factor of neural progenitors, human MGSCs (hMGSCs) can be induced to differentiate into an enriched cell population expressing markers of RGC precursors,

including BRN3B, HUD, and ISL-1 [6, 7]. These cells also display neural function in vitro, as judged by their responsiveness to nicotine, a neurotransmitter known to stimulate RGC precursors [6, 8]. Following intravitreal injection of hMGSCs-derived RGCs into a rat model of RGC depletion, transplanted cells attached to the inner retina and significantly improved visual function despite not extending axons to the optic nerve [6]. This was demonstrated by a partial but significant recovery of the negative component of the scotopic threshold response (STR) of the electroretinogram (ERG), an indicator of RGC function [9, 10]. These findings have prompted us to further investigate and refine methods for retinal cell delivery that not only could advance our transplantation approaches but that also could have translational potential for cell-based therapies to treat patients affected by glaucoma.

When designing protocols for retinal cell transplantation, the anatomical differences between species should be considered because they will determine the development of appropriate methods for cell transplantation. Most studies undertaken in the transplantation field have used the small rodent eye as a model for neural stem cell grafting. However, the rat and mouse eyes exhibit a relatively large lens with a very small vitreous volume, and therefore the lens may serve as a scaffold to facilitate retinal attachment and integration of cells injected into the vitreous [11]. In contrast, the human eye has a larger vitreous cavity with a relatively small crystalline lens. Consequently, methods successfully used for transplantation of RGC onto the inner rat retina may not be directly applicable to humans. In order to translate these findings toward clinical use, it is necessary to investigate animal models that more closely resemble the anatomical features of the human eye. We hypothesize that because of the anatomy of the large mammalian eye, efficient transplantation of RGCs into the human eye may be aided by direct cell grafting onto the inner retinal surface, which may require the use of cellular scaffolds to support cell attachment and survival.

Because the feline eye exhibits many of the anatomical and physiological characteristics of the human eye, it constitutes an appropriate model in which to undertake translational studies aimed at developing human therapies to restore visual function [12]. On this basis, we investigated methods for the delivery of RGCs into the cat eye. Taking into account that immune reactivity to grafted cells represents an additional barrier to transplant integration and survival and that a severe reaction to human cells was observed in our initial investigations, to avoid xenogeneic reactivity we derived MGSCs from the cat retina for the study. A population of Müller glia isolated from the cat retina was examined for the expression of Müller cell and progenitor markers as previously reported in the human eye [5]. Feline Müller glia exhibiting key stem cell features, like those seen in hMGSCs, were differentiated into an enriched cell population exhibiting markers of RGCs before transplantation onto the inner cat retina that had been depleted of RGCs by *N*-methyl-D-aspartate (NMDA). Transplantation was undertaken by either intravitreal injection of a cell suspension or by transplantation of cells attached to collagen scaffolds in the vitrectomized eye to promote cell attachment onto the inner retina. The outcome of the transplantation was assessed by ocular coherence tomography (OCT), immunohistochemical analysis of the transplanted retina in vitro, and assessment of the RGC function by ERG in vivo.

MATERIALS AND METHODS

Isolation and Characterization of Müller Glial Cells With Progenitor/Stem Cell Characteristics From the Feline Eye

Müller glial cells were isolated from the adult retina of domestic feline eyes supplied by Matrix Biologicals Ltd. (Humberstone, U.K., <http://www.matrixbiologicals.co.uk>) using methods previously established in our laboratory for the isolation of these cells from the adult human eye [13]. Briefly, after removal of the vitreous, the neural retina was carefully dissected from the retinal pigment epithelium and digested at 37°C for 20 minutes using 0.01% trypsin/EDTA. Following mechanical dissociation of these cells by vigorous pipetting, the cells were washed three times with Dulbecco's modified Eagle's medium (DMEM) cell culture, followed by culture in DMEM supplemented with GlutaMAX (Gibco, Life Technologies, Grand Island, NY, <http://www.invitrogen.com>), 10% fetal bovine serum (FBS; Gibco, Life Technologies), 40 ng/ml epidermal growth factor (Sigma-Aldrich, St. Louis, MO, <http://www.sigmaproducts.com>), 20 U/ml penicillin, and 20 µg/ml streptomycin (Gibco, Life Technologies). The cells were plated onto 12.5-cm² tissue culture dishes coated with fibronectin and incubated for 3–4 weeks until formation of adherent cell colonies. To passage cells, confluent monolayers were detached once a week using TrypLEExpress (Gibco, Life Technologies) and subcultured at a dilution of 1:5. For transplantation, cells were used from passages 25 to 31, and for in vitro characterization studies, they were used between passages 9 and 35. Upon confluence, cells were examined for markers of both Müller glia (vimentin, glutamine synthetase, and cellular retinaldehyde binding protein [CRALBP]) and neural progenitor cells (Sox2, Pax6, and Notch) as previously described [5]. Isolated feline Müller glia, cells were cultured on flasks coated with basement membrane protein (BMP; Sigma-Aldrich) with DMEM containing 2% FBS supplemented with 20 ng/ml basic fibroblast growth factor-2 (FGF-2; PeproTech, Rocky Hill, NJ, <http://www.peprotech.com>) and 50 µM *N*-(*N*-(3,5-difluorophenylacetyl)-L-alanyl)-S-phenylglycine *t*-butyl ester (DAPT; Sigma-Aldrich) for 7 days, a protocol previously described for RGC differentiation of hMGSC [6]. Confirmation of differentiation was assessed by downregulation of the Notch signaling molecule Hes1 and expression of Brn3b, a RGC marker [6].

RNA Isolation and Reverse Transcription-PCR Analysis

Total RNA was isolated from cell pellets of cultured feline Müller cells using the RNeasy system (Qiagen, Hilden, Germany, <http://www.qiagen.com>). For reverse transcription, 500 ng of RNA in 11 µl of RNase-free water was incubated in an Eppendorf Mastercycler gradient (Eppendorf AG, Hamburg, Germany, <http://www.eppendorf.com>) with 0.5 µg of oligo(dT)_{12–18} primers (Life Technologies) and 0.5 mM dNTPs (Life Technologies) in a total volume of 20 µl at 65°C for 5 minutes. Following addition of 5 mM DTT, 40 U of RNasin Plus (Promega, Madison, WI, <http://www.promega.com>) and 200 U of Superscript III (Invitrogen) in first strand buffer, cDNA was generated by incubation at 50°C for 60 minutes, and the reaction was stopped by heating to 70°C for 15 minutes. Polymerase chain reaction (PCR) amplification was performed using primers derived from the GenBank database (sequences shown in supplemental online Table 1). Amplification was performed using 2 µl of cDNA, with 12.5 µl of GoTaq Mastermix (Promega), 8.5 µl of RNase-free water, and 1 µl of each forward and reverse primers.

The mixture was incubated at 95°C for 2 minutes, followed by 24–38 cycles (depending on the primers used) as follows: 95°C for 1 minute, 60°C for 1 minute, 72°C for 1 minute, and 1 cycle of 72°C for 5 minutes. Primers were optimized to ensure that signals derive only from the exponential phase of amplification. PCR products were analyzed by agarose gel electrophoresis (2%) containing 1:15,000 Gel Red (Biotium; Cambridge Bioscience, Cambridge, U.K., <http://www.bioscience.co.uk>).

Western Blotting Analysis

Cell lysis and Western blot analysis was performed as previously described [5]. Briefly, 10 µg of protein from cell lysates containing protease inhibitors were resolved on 4%–8% Bis-Tris Invitrogen NuPage gels in MOPS running buffer (50 mM MOPS, 50 mM Tris base, 0.1% SDS, 1 mM EDTA [pH 7.7]; Invitrogen) for 60 minutes at 180 V. Proteins were transferred to polyvinylidene difluoride membranes using a semidry transfer apparatus (Bio-Rad, Hercules, CA, <http://www.bio-rad.com>) and run for 30 minutes at 25 V. The membranes were blocked with 5% nonfat milk powder and 5% FBS in phosphate-buffered saline (PBS) containing 0.1% Tween 20. Immunodetection was performed using various monoclonal and polyclonal antibodies as listed in supplemental online Table 2. Immunocomplexes were detected by enhanced chemiluminescence (Amersham Biosciences, Piscataway, NJ, <http://www.amersham.com>) following incubation with goat or donkey antiserum against rabbit, sheep, or mouse IgG coupled to horseradish peroxidase (Jackson ImmunoResearch Laboratories, Bar Harbor, ME, <https://www.jax.org>) diluted 1:5,000 in Tris-buffered saline (TBS) containing 0.1% Tween-20. Images were analyzed and processed using a Fuji image reader LAS-1000 Pro, version 2.1 (Fuji, Bedford, U.K., <http://www.fujifilm.eu/uk>).

Animal Husbandry, Immunosuppression, and Anesthesia

Female domestic short-haired cats (2–4 kg of body weight) were purchased from Isoquimen (Barcelona, Spain, <http://www.isoquimen.com>). The animals were maintained according to the U.K. Home Office regulations for the care and use of laboratory animals (Scientific Procedures Act 1986). The use of the animal species for the study was approved by the local ethics committee at the University College London Institute of Ophthalmology and the U.K. Home Office. The animals were given access to food and water ad libitum and kept under 12-hour light/12-hour dark cycles. Immunosuppression, consisting of 1 mg/kg prednisolone and 10 mg/kg cyclosporine A, administered orally twice daily, was induced 48 hours prior to transplantation and continued for the first week after transplantation. Thereafter, cyclosporine A was continued at the same dose, but prednisolone was reduced to 0.5 mg/kg, twice daily for up to 2 weeks until termination of the experiment. For surgical procedures and ERG recordings, the cats were anesthetized by i.m. injection of 5 mg/kg ketamine, 0.4 mg/kg butorphanol, and 80 µg/kg medetomidine. For OCT imaging, the cats were lightly sedated using i.m. injection of 0.2 mg/kg butorphanol and 40 µg/kg medetomidine. Only one eye was treated in each animal, with the untreated eye serving as a control.

Immunocytochemistry and Confocal Microscopy

For immunocytochemistry, feline Müller glia were cultured for up to 7 days on Lab-Tek Permanox Chamber Slides (Nunc, Rochester, NY, <http://www.nuncbrand.com>) coated with BMP (10 µg/ml) in the presence or absence of differentiation factors (as above),

followed by fixation with 4% paraformaldehyde in PBS for 10 minutes and cryopreservation with 30% sucrose in PBS for 10 minutes. The slides were dried at room temperature and kept at –20°C until use. Cryostat sections of retinal tissues (10-µm thickness) were fixed and cryopreserved as above. Prior to immunostaining, slides containing cells and tissue sections were thawed and rinsed with PBS (pH 7.2), and immunocytochemistry was performed as previously described [6]. Negative controls omitting the primary antibody were used throughout the experiments. Primary antibodies used are listed in supplemental online Table 2. After incubation with primary antibodies, specimens were washed in TBS, followed by 2-hour incubation with Alexa Fluor 488- or 555-conjugated secondary antibodies (Invitrogen). The slides were washed, counterstained with 2 µg/ml 4',6'-diamino-2-phenylindole (DAPI) (1:5,000 in TBS) for 1 minute and mounted with Vectashield mounting medium (Vector Laboratories, Burlingame, CA, <http://www.vectorlabs.com>). Fluorescent images were recorded using a Zeiss LSM 710 confocal microscope operating in multitrack mode for the different fluorochromes.

Preparation of Cells for Transplantation

For initial studies investigating intravitreal injection of hMSGCs, we used the MIO-M1 cell line that had been transfected with lentiviral enhanced green fluorescent protein (eGFP), cultured, and differentiated into RGCs as previously described [6]. To facilitate the tracking of the transplanted cat cells, fMGSCs were transfected with eGFP lentiviral particles (GeneCopoeia, Rockville, MD, <http://www.genecopoeia.com>; LabOmics, Nivelles, Belgium, <http://labomics.com>) using previously described methods [6]. Briefly, cells cultured at a 50% confluence in a 24-well plate were transfected with 5×10^8 particles. Using this method, more than 90% of Müller cells expressed GFP 1 week after transfection. Lentiviral transfected cells were grown to confluence in a 25-cm² flask, and GFP⁺ cells were selected by fluorescence-activated cell sorting cell sorting using a FACScalibur flow cytometer (BD Biosciences, San Diego, CA, <http://www.bd biosciences.com>). To ensure that the lentiviral vector did not modify the stem characteristics of the transfected cells, they were examined for the expression of Müller glia and stem cell markers as previously described [5]. There was no evidence of the lentiviral eGFP reporter being shed from the cells following multiple fMGSC cell divisions and during RGC differentiation in vitro. For transplantation, cells were differentiated into enriched populations of RGCs following Notch downregulation by DAPT and FGF-2 (as described above). For clarity, we have referred to these cells as fMGSC-RGCs. On the day of transplantation, cells were detached, washed, and resuspended in serum-free DMEM. The cells were transplanted as a 50-µl suspension containing 5×10^5 cells and 0.2 U of chondroitinase ABC (ChABC; Seikagaku, Tokyo, Japan, <http://www.seikagaku.co.jp>; supplied by AMS Biotechnology, Abingdon, U.K., <http://www.amsbio.com>).

Preparation of Compressed Collagen Membranes for the Design of Cellular Scaffolds for Transplantation

As previously reported [14, 15] and illustrated in supplemental online Figure 1, 300 µl of a neutralized 0.75% rat tail type I collagen solution (FirstLink) was added to circular titanium molds (1 cm in diameter = 0.78 cm²) and incubated at 37°C in 5% CO₂ for up to 30 minutes to induce fibrillogenesis. Hydrogels were placed between nylon meshes and compressed with 150 g of weight for 5 minutes. The resulting collagen scaffolds were

washed with phosphate-buffered saline and placed over the well of 35-mm glass bottom culture dishes (20-mm glass diameter) (MatTek, Ashland, MA, <https://www.mattek.com>) with 150 μ l of a suspension containing 3×10^5 fMGSC-RGCs in DMEM with 5% FBS. To ensure that cells adhered to both surfaces of the collagen mats, an additional 150 μ l of the same cell suspension were placed over the mats, which were then incubated for 60–90 minutes at 37°C. Collagen mats containing the adherent cells (cellular scaffolds) were briefly rinsed in sterile saline solution for injection and placed in an 18-gauge cannula attached to a 1-ml syringe immediately before transplantation. All procedures leading to the preparation of the scaffolds were performed aseptically.

Induction of RGC Death by NMDA in the Feline Eye and Transplantation of fMGSC-RGCs

NMDA injections were administered under direct visualization of the fundus through the pharmacologically dilated pupil using an operating microscope. The dorsolateral conjunctiva was dissected from the underlying sclera, and a 33-gauge metal needle attached to a glass Hamilton syringe containing the materials to be injected was inserted into the intravitreal space adjacent to the inner retinal surface (avoiding injury to the lens). In order to induce RGC damage as previously shown [16–19], animals received an intravitreal injection of 33 or 50 μ l of a stock solution containing 80 mmol/l INMDA in sterile injectable saline. By estimating the volume of the feline vitreous as 2.7 ml, the final concentrations of NMDA injected were 1.0 and 1.5 mmol/l, respectively. As previously reported, to avoid excessive microglia accumulation associated with NMDA-induced RGC death [17], we injected 0.5 mg of triamcinolone (TA) together with NMDA. Retinal function was assessed at 1–2 weeks after NMDA and TA injection by measurement of the STR and photopic negative response (PhNR) of the ERG.

The animals were transplanted with cell suspensions of either hMGSC-RGCs (2 animals) or fMGSC-RGCs (1 animal), or cells adhered to collagen scaffolds (9 animals) prepared as indicated above, 1–2 weeks after NMDA/TA injection. Intravitreal transplantation of RGC suspensions was performed by injection through the pars plana using a 23-gauge cannula. The cells were resuspended in 50 μ l containing 0.2 U of ChABC as indicated above and injected onto the inner retinal surface, either in nonvitrectomized or vitrectomized animals. For the transplantation of fMGSC-RGCs adhered to collagen scaffolds, the animals were subjected to a pars plana vitrectomy and lensectomy as previously described [11]. Following fluid-air exchange, cellular scaffolds were placed into an 18-gauge cannula for delivery onto the inner retinal surface of the central retina together with 0.2 U of ChABC (protease-free; Seikagaku, supplied by AMS Biotechnology).

OCT Imaging and ERG Recordings

Localization of the transplanted cellular scaffolds was evaluated using confocal scanning laser ophthalmoscopy and Fourier domain OCT (Spectralis HRA+OCT; Heidelberg Engineering, Heidelberg, Germany, <http://www.heidelbergerengineering.com>). To assess attachment of cellular scaffolds and cell migration after transplantation, high resolution line scans were acquired across the area centralis (where the transplants were placed). Animals were sedated as described above, pupils were dilated using phenylephrine and tropicamide eye drops, and topical anesthesia to the corneal surface was applied using tetracaine eye drops. During the imaging procedure, animals were placed on a heated surface to regulate

their body temperature. Autofluorescence and SD-OCT images were gathered at wavelengths of 488 and 870 nm, respectively.

For the recording of ERGs, cats were dark-adapted for 1–2 hours and subsequently handled under dim red light illumination. The animals were sedated as described above and placed on a heated table to control the body temperature in a Ganzfeld stimulator (Color-dome; Diagnosys, Cambridge, U.K., <http://diagnosysllc.com>). Subdermal ground and reference electrodes were inserted near the posterior region of the hindquarter and near the outer canthi, respectively. Active electrodes (ERG jet electrodes; Fabrinal, La Chaux-de-Fonds, Switzerland, <http://fabrinal.ch>) were placed onto the corneas, which were lubricated with Viscotears (Novartis International, Basel, Switzerland, <http://www.novartis.com>). ERGs were recorded using Espion (Diagnosys) software and stored on a PC for off-line analysis. Scotopic ERG responses were recorded on presentation of a series of light flashes of intensity 10^{-8} – 10 cd·s·m $^{-2}$, with interflash intervals of 7.5–20 seconds and 25–3 recordings per condition acquired and averaged depending on the light intensity (supplemental online Table 3). The STR, which has been reported to originate in the RGC layer and to be an estimate of RGC function [9, 20], was measured without contributions from other retinal neurons at flash intensities of $10^{-5.5}$ and 10^{-5} cd·s·m $^{-2}$. The PhNR was recorded after 10 minutes of light adaptation on a yellow background (35 cd·s·m $^{-2}$) using blue light flashes (0.01 – 3.5 cd·s·m $^{-2}$), as previously reported [21, 22] (supplemental online Table 3).

Statistical Analysis

The data are presented as means \pm SEM. Statistical analysis was performed by *t* test or two-way analysis of variance with a Bonferroni post hoc test, as appropriate. The null hypothesis was rejected for $p < .05$, and statistically significant differences are indicated by asterisks.

RESULTS

Isolation of fMGSCs and Examination of Their Ability to Differentiate Into RGCs

Müller glial cells with stem cell characteristics were isolated from the feline retina using standard protocols for isolation of hMGSCs [5, 13]. Like hMGSCs, feline Müller glia exhibited a characteristic glial bipolar morphology and consistently proliferated above 30 passages. They expressed mRNA coding for transcription factors of neural progenitors, including *Notch*, *Hes1*, *Sox2*, *Pax6*, and β *III-tubulin* (Fig. 1A), as well as mRNA coding for *vimentin*, a well-known glial marker. Because of the nonavailability of antibodies to feline species, we stained these cells with antibodies to human Müller glia markers, which showed cross-reactivity. These included CRALBP, vimentin, and glutamine synthetase (Fig. 1A). Feline Müller glia that expressed markers of neural progenitors were induced to differentiate into RGCs by inhibition of Notch signaling using a previously published protocol to induce RGC differentiation of hMGSCs [6]. As observed with hMGSCs, Notch inhibition by FGF-2/DAPT caused morphological changes in feline Müller glia, identified on light microscopy by the acquisition of long cytoplasmic projections, which gave the appearance of neural-like morphology (Fig. 1B). Furthermore, feline Müller glia undergoing Notch downregulation showed a marked decrease in immunostaining intensity with antibodies to the full length of human Notch, indicating a reduced expression of this intracellular protein. This was accompanied by a clear reduction in vimentin

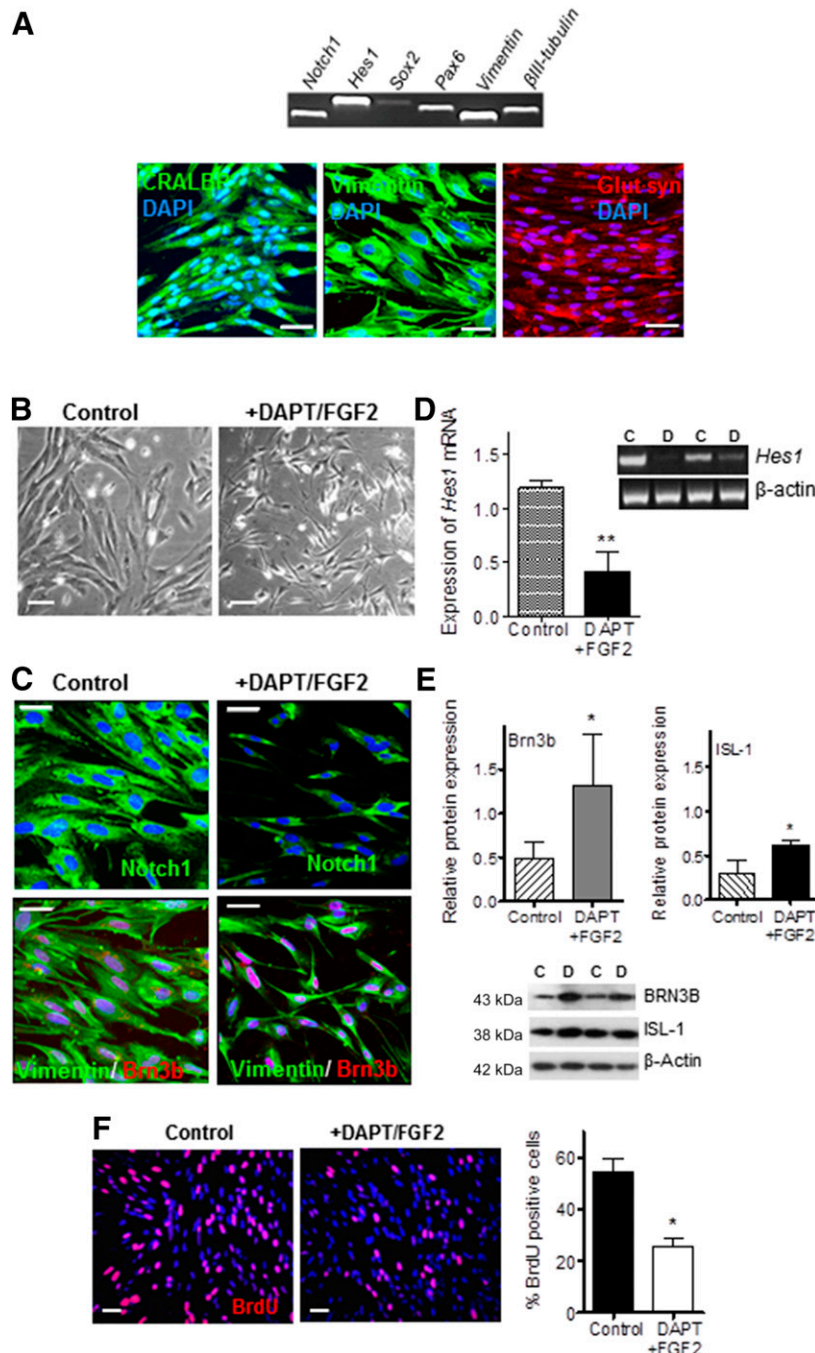


Figure 1. Characterization of feline Müller glia with stem cell properties. **(A)**: Müller glia derived from the feline eye that proliferated extensively in culture express mRNA coding for markers of neural progenitors, including *Notch*, *Hes1*, *Sox2*, *Pax6*, and β *III*-*tubulin*, as well as *vimentin*, a known marker of Müller glia. Immunostaining of cells in culture showed that these cells express CRALBP (Alexa 488, green), vimentin (Alexa 488, green), and glutamine synthetase (Alexa 555, red). Scale bars = 50 μ m. **(B)**: Phase contrast photomicrographs of feline Müller glia in culture (passage 8) showed that these cells exhibited characteristic bipolar morphology. Downregulation of Notch by DAPT and FGF-2 induced these cells to acquire long cytoplasmic processes resembling a neural-like morphology. Scale bars = 50 μ m. **(C)**: As judged by immunostaining, feline Müller glia cultured with DAPT and FGF-2 exhibited a reduced expression of Notch1 and Vimentin (Alexa 488, green), when compared with the controls. Nuclear staining of the transcription factor Brn3b was also increased (Alexa 555, red). Scale bars = 50 μ m. **(D, E)**: Notch downregulation also caused a decrease in mRNA coding for *Hes1*, a downstream factor of Notch signaling, concomitant with an increase in Brn3b and *Isl1* protein expression as seen by Western blotting (**, $p < .02$; $n = 3$). **(F)**: The percentage of proliferating cells as determined by BrdU⁺ incorporation (Alexa 555, red) was significantly reduced following Notch downregulation (*, $p < .05$; $n = 3$). Scale bars = 50 μ m. Cell nuclei counterstained with DAPI (blue). Bars on histograms indicate means \pm SEM of three different experiments. Abbreviations: BrdU, bromodeoxyuridine; C, control; CRALBP, cellular retinaldehyde binding protein; D, differentiated; DAPI, 4',6'-diamino-2-phenylindole; DAPT, N-[N-(3,5-difluorophenacetyl)-L-alanyl]-S-phenylglycine t-butyl ester; FGF, fibroblast growth factor; Glut syn, glutamine synthetase.

staining and a concomitant upregulation of the intensity of nuclear staining for Brn3b, a marker of RGCs (Fig. 1C). As seen with hMGSCs, a decrease in mRNA coding for *Hes1*, a downstream factor of the *Notch* signaling pathway, was also observed in cells treated with FGF-2/DAPT (Fig. 1D). Although the proportion of Brn3b-positive cells detected with the antibody to human Brn3b was similar in both fMGSCs treated with DAPT/FGF2 and control cells (60%–65%), the intensity of staining for this molecule was noticeable higher in the differentiated cells (Fig. 1C). In addition, Western blot analysis of cell lysates from feline Müller glia treated with FGF-2/DAPT showed an increase in the expression of *Isl-1* and Brn3b as judged by Western blotting (Fig. 1E). Cell proliferation, as assessed by bromodeoxyuridine staining, was significantly reduced by *Notch* inhibition in comparison with control cells (*, $p < .05$, $n = 395$ and 405 from 3 separate experiments, respectively) (Fig. 1F). This is in agreement with previous findings in hMGSCs that RGC differentiation is accompanied by a decrease in cell proliferation [6]. Based on these observations, it can be concluded that Müller glia isolated from the feline retina that proliferate extensively, express neural progenitor markers, and differentiate into RGC in vitro constitute a population of Müller glia with stem cell characteristics, for which we named them feline Müller stem cells (fMGSCs).

Induction of RGC Damage by NMDA in the Feline Retina

Previous studies have demonstrated that NMDA reduces RGC function as measured by electroretinography in the rodent [17, 23, 24] and cat retina [19]. Although spontaneous and genetic feline glaucoma models exist [25], they result in variable degrees of slowly progressive RGC damage that are less desirable for short-term investigations than RGC damage induced by intravitreal injection of NMDA. The concentrations used in the present study were aimed at causing only partial impairment of RGC function, which could be monitored to assess any improvements of retinal function by cell transplantation. The results showed that the STR of the dark-adapted ERG was not significantly affected by injection of 1.0 mmol/l NMDA ($p > .05$; $n = 4$; Fig. 2A). However, injection of 1.5 mmol/l NMDA induced a significant reduction of both the STR at light intensities of $10^{-5.5}$ and 10^{-5} cd·s·m $^{-2}$ (*, $p < .05$ and **, $p < .01$, respectively; $n = 4$; Fig. 2B), as well as the PhNR at light intensities between 1 – 3.5 cd·s·m $^{-2}$ (*, $p < .05$ at 1 and 2 cd·s·m $^{-2}$; **, $p < .01$ at 3 and 3.5 cd·s·m $^{-2}$; $n = 4$; Fig. 2C), indicating a decrease in the RGC function. ERG testing over a range of light intensities (10^{-4} – 2 cd·s·m $^{-2}$) in the dark-adapted state showed that the a- and b-waves of the scotopic ERG remained unaffected by intravitreal injection of 1.5 mmol/l NMDA (Fig. 2D), suggesting that other retinal neurons such as photoreceptors and bipolar cells remained largely unaffected by treatment with NMDA. Although the NMDA concentrations necessary to induce significant attenuation of the RGC-dependent components of the ERG were slightly higher than previously reported in the cat [19], those used in rodent models in other studies varied widely [17, 23, 24]. Our findings that both the STR and PhNR were significantly reduced by treatment with 1.5 mmol/l NMDA are consistent with the view that both responses are largely attributed to RGC function and that they can be depressed by glaucomatous damage [26–29].

Intravitreal Transplantation of Enriched Preparations of hMGSC-RGCs Causes Severe Inflammation in the Feline Eye

Two weeks after intravitreal injection of 1.5 mmol/l NMDA/TA, a suspension containing 5×10^5 hMGSC-RGCs (~60% RGC) and 0.2

U of ChABC to promote cell migration into the retina [7] was transplanted in two animals by intravitreal injection close to the inner retinal surface. Assessment of retinal function by ERG and histological analysis of the transplanted eye were performed 2 weeks after cell injection. Confocal microscopy examination of the transplanted eyes showed that grafted hMGSC-RGC preparations formed large aggregates within the vitreous, which were clearly seen at the vitreous base adjacent to the ciliary body only (Fig. 3A). Interestingly, transplanted cells that did not aggregate were observed migrating and attaching to the ciliary processes of the ciliary epithelium (Fig. 3B). Unlike previous observations in the rat eye after intravitreal transplantation of a suspension of hMGSC-RGC [6], human cells injected into the feline vitreous did not migrate into the RGC layer or attach onto the inner retinal surface. Typically, grafted cells formed large aggregates within the vitreous body (Fig. 3C). Despite systemic immunosuppression, these cell aggregates were surrounded by immune reactive microglia, as evident by the capping of isolectin B4-positive cells around the transplanted cells (Fig. 3C). The lack of cell migration into the retina and the inflammatory response triggered by the transplanted cells were reflected in their failure to improve the STR, an electrophysiological indicator of RGC function in animals depleted of RGC by NMDA (Fig. 3D, 3E).

Intravitreal Transplantation of Cell Suspensions of fMGSC-RGCs Into the Feline Eye

To minimize the severe inflammatory response caused by xenogeneic transplantation of hMGSC-RGCs into the feline eye despite systemic immunosuppression, we performed a preliminary experiment to assess whether transplantation of cell suspensions in the vitrectomized eye could be feasible. For this investigation, fMGSCs that had been induced to express markers of RGCs were subsequently injected into the vitreous of a single cat eye depleted of RGCs by a 1.5 mM NMDA/TA injection. Two weeks after intravitreal injection of NMDA/TA, we performed a partial vitrectomy using a previously optimized protocol in our laboratory [11]. A suspension of 5×10^5 feline cells expressing RGC markers (~60% RGCs) and 0.2 U of ChABC was injected through the vitrectomy port under direct visualization onto the posterior pole of the feline retina. Histological and functional assessments of the transplant were performed 2 weeks after transplantation. Protocols used for cell transplantation are illustrated in supplemental online Figure 1.

Macroscopic examination of the dissected eye showed that despite vitrectomy and transplantation of allogeneic cells, pronounced aggregation of the transplanted cells was observed, possibly caused by entrapment of cells in vitreous remnants not removed by vitrectomy (Fig. 4A). Histological analysis of transverse sections of the area where cell aggregates were observed macroscopically showed severe accumulation of microglia surrounding the transplanted eGFP $^+$ cells. This microglia reactivity was determined by immunoreactivity to lectin B4 (Fig. 4B). Despite the lack of integration of the transplanted cells and the inflammatory response observed, we saw a slight improvement of the STR in the transplanted eye as compared with the STR before transplantation but after the NMDA treatment (Fig. 4C).

Transplantation of Cellular Scaffolds Onto the Inner Surface of the Feline Retina

In order to prevent cell aggregation and improve cell attachment of the transplanted cells onto the retina, we prepared cellular scaffolds of compressed collagen using a modification of a

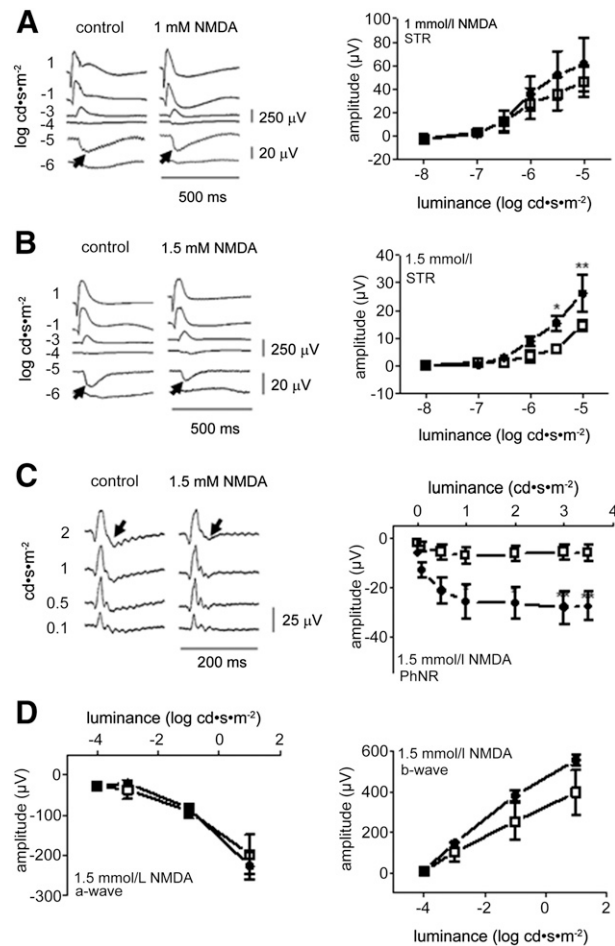


Figure 2. Responses of the electroretinogram (ERG) to injection of NMDA into the feline vitreous. **(A)**: Representative traces and mean STRs of the ERG to injection of 1 mmol/l NMDA into the feline vitreous. The STR was not significantly affected by this dose of NMDA in comparison with the control eye (filled circles). STR is indicated by arrows. **(B)**: Representative images and mean STR responses to intravitreal injection of 1.5 NMDA. The amplitude of the STR was significantly reduced by this dose of NMDA at flash intensities of $10^{-5.5}$ and 10^{-5} $\text{cd}\cdot\text{s}\cdot\text{m}^{-2}$ (empty squares; *, $p < .05$; **, $p < .01$; $n = 4$) as compared with the control eye (filled circles). STR is indicated by arrows. **(C)**: Typical example traces and mean PhNR of the ERG to intravitreal injection of 1.5 mmol/l NMDA. The amplitude of the PhNR was significantly attenuated by injection of 1.5 mmol/l NMDA at flash intensities of $1-3.5$ $\text{cd}\cdot\text{s}\cdot\text{m}^{-2}$ (empty squares; *, $p < .05$; **, $p < .01$; $n = 4$) in comparison with the control eye (filled circles). PhNR is indicated by arrows. **(D)**: The amplitudes of the scotopic a- and b-waves remained unaffected by intravitreal injection of 1.5 mmol/l NMDA (empty squares; $p > .05$; $n = 4$) in comparison with the control eye (filled circles) at flash intensities ranging from 10^{-4} to 10^1 $\text{cd}\cdot\text{s}\cdot\text{m}^{-2}$. Effective concentrations of NMDA are given after intravitreal injection. Bars on each point of the luminance curves indicate means \pm SEM of three different experiments. Arrows indicate the implicit times at which the STR and PhNR were analyzed. Abbreviations: NMDA, *N*-methyl-D-aspartate; PhNR, photopic negative response; STR, scotopic threshold response.

published method [14, 15] and illustrated in Materials and Methods (supplemental online Figure 2). Following pars plana vitrectomy [11], cellular scaffolds were transplanted through the vitrectomy port with 0.2 U of ChABC onto the inner retinal surface of the feline eye, using a 18-gauge cannula (Fig. 5A). Scaffolds were placed adjacent to the posterior pole. At 1 and 2 weeks after transplantation, the migration of eGFP⁺ cells from the scaffold

onto the inner retinal surface was assessed by OCT, whereas RGC function was assessed by ERG. The animals were then sacrificed, and their eyes were enucleated for histological examination of the transplanted retina.

OCT images of transplanted retina showed that 1 week after transplantation, cellular scaffolds were closely apposed to the inner retinal surface (Fig. 5B). Detailed evaluation of infrared confocal ophthalmoscopy en face images of the retina and scaffold indicated that cells attached to the collagen membranes were migrating along the retinal surface, some of which appeared to have migrated away from the scaffold and displayed elongated cellular processes resembling neuronal processes (Fig. 5C). Furthermore, OCT images showed that cells migrating away from the scaffolds were extending across the optic nerve head surface but not into the nerve head itself (Fig. 5E).

Histological examination of the transplanted retina at 2 weeks after transplantation of cellular scaffolds confirmed the attachment of transplanted cells onto the inner retinal surface. However, histological sections showed that cellular scaffolds were detached from the retina (Fig. 6A, 6C, 6D), and cells were observed to have migrated from the scaffold onto the inner retinal surface. Cells that attached onto the surface of the optic nerve head did not migrate into the optic nerve itself (Fig. 6B). Overall, cell attachment onto the retina appeared to be confined to the region where the scaffold was placed (Fig. 6C, 6D). Based on the OCT images obtained *in vivo*, the scaffold detachment observed histologically may have occurred *ex vivo* as a result of retinal tissue processing, fixation, and sectioning.

Following NMDA-induced RGC damage, transplantation of fMGSC-RGCs on cellular scaffolds was associated with significant improvement of RGC function in the same eye as measured by ERG at 2 weeks after transplantation. As shown in Figure 7A, the amplitude of the STR at a light intensity of $10^{-5.5}$ $\text{cd}\cdot\text{s}\cdot\text{m}^{-2}$ was increased from 50.3% in the uninjected control eye after NMDA injection alone to 70.3% (*, $p < .05$) after NMDA injection and cell transplantation. No significant alterations of the a- and b-waves of the ERG were observed after cell transplantation with all light intensities tested ($p > .05$; $n = 3$; Fig. 7B). Similarly, following NMDA injection and transplantation of cellular scaffolds, the amplitude of the PhNR was improved at light intensities of 1 and 3 $\text{cd}\cdot\text{s}\cdot\text{m}^{-2}$, with an increase from a median value of 15.5% in the NMDA only treated eyes to 67.5% in eyes subjected to NMDA and cellular scaffold transplantation at 3 $\text{cd}\cdot\text{s}\cdot\text{m}^{-2}$ (*, $p < .05$; $n = 4$; Fig. 7C).

DISCUSSION

Development of stem cell transplantation protocols for replacement or neuroprotection of damaged RGCs may constitute a therapeutic approach for patients with advanced glaucoma for whom conventional treatments are not effective [30, 31]. Local engraftment into the RGC layer of retinal progenitors derived from mouse [32] and human [33] embryonic stem cells using mouse models of optic nerve damage has been documented, although no observations have been made of transplanted cells forming nerve fibers projecting into the optic nerve [32, 33]. Adult-derived hMGSCs [5], which are competent to differentiate toward a functional RGC phenotype [6, 34], are able to adhere to the inner retina and to migrate at the site of the transplant into the RGC layer of a rat model of RGC depletion [6, 17]. Although transplanted cells were not seen to extend long axons into the optic nerve, they were

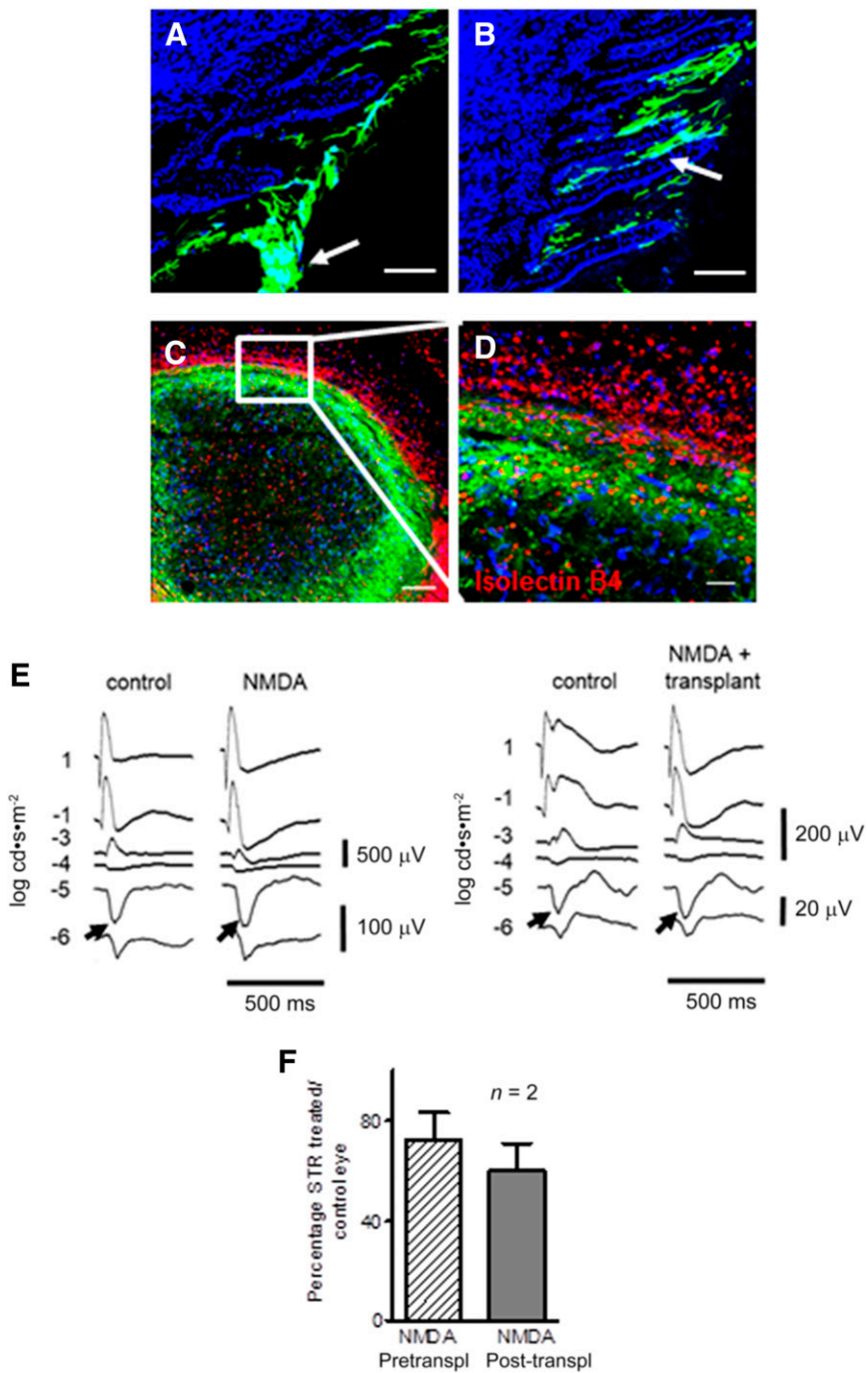


Figure 3. Histological and electrophysiological responses to cells transplanted in suspension. **(A)**: Human Müller glia-derived-retinal ganglion cells (RGCs) (green fluorescence) injected into the vitreous of the feline eye depleted of RGCs by NMDA formed large aggregates in the region adjacent to the ciliary body (white arrow). Scale bar = 100 μ m. **(B)**: Nonaggregated cells were also observed migrating and attaching to the ciliary processes of the ciliary epithelium (white arrow). Scale bar = 100 μ m. **(C)**: Large cell aggregates observed in the vitreous adjacent to the anterior retina were surrounded by microglia as judged by immunostaining for isolectin B4 (Alexa 555, red). Scale bar = 100 μ m. **(D)**: Magnification of the section marked by the white square in **(C)**. Scale bar = 20 μ m. Electrotoretinogram (ERG) traces show that 2 weeks after cell transplantation, the STR of the ERG did not show any significant changes at a light intensity of 10^{-5} $cd\cdot s\cdot m^{-2}$ in the transplanted eye when compared with eyes that had undergone NMDA injection alone. STR is indicated by arrows. **(E)**: Histogram shows the mean amplitude of the STR \pm SEM of the NMDA-treated eyes before and after cell transplantation as percentages of the control eyes ($n = 2$). Cell nuclei counterstained with 4',6'-diamino-2-phenylindole (blue). Abbreviations: NMDA, *N*-methyl-D-aspartate; Post-transpl, post-transplantation; Pretranspl, pretransplantation; STR, scotopic threshold response.

shown to establish synapses with local neurons at the site of transplantation, and more importantly, they were able to improve the RGC function as measured by the STR response of the ERG [6].

Taking into consideration the anatomical and physiological differences in the eye between species, it is important to validate transplantation techniques in experimental models that more closely

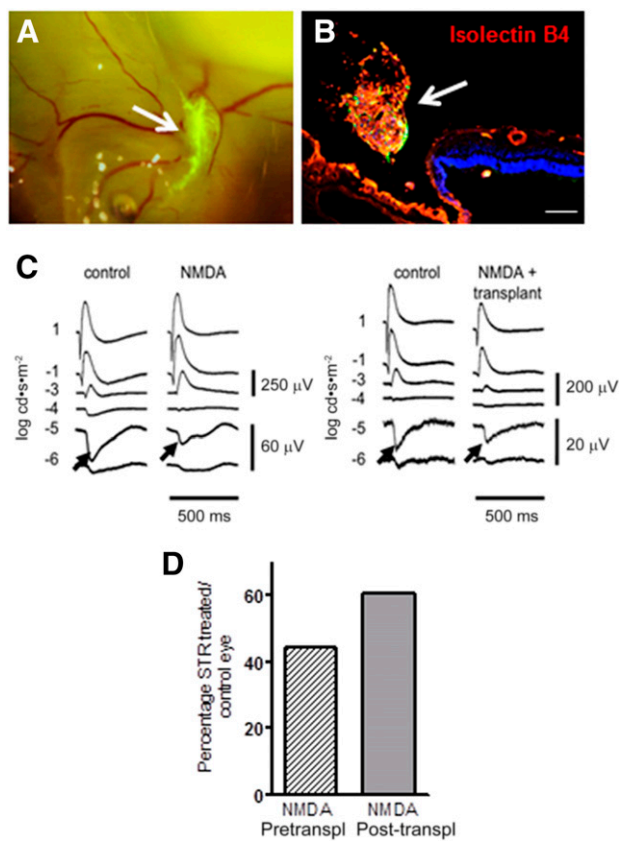


Figure 4. Histological and electrophysiological responses to a cell suspension transplanted into the vitrectomized eye. **(A)**: Fluorescent dissecting microscope image of an eye that had been subjected to retinal ganglion cell (RGC) depletion by 1.5 mmol/l NMDA, followed by vitrectomy and subsequently transplanted with a suspension of 6×10^5 RGCs derived from feline Müller glial stem cells. Cell aggregates (green) can be clearly observed in the small fragments of remaining vitreous (arrow). **(B)**: Microscopic examination of the same eye showing large cell aggregates (green) in the inferior nasal region surrounded by microglia, as determined by immunostaining for isolectin B4 (Alexa 555, red) (arrow). **(C)**: Electroretinogram (ERG) traces of the scotopic flash ERG showed a minor improvement in the eye injected with the cell suspension at 2 weeks post-transplantation. STR is indicated by arrows. **(D)**: This improvement was more clearly seen by plotting the amplitude of the STR response of the NMDA-treated eye before and after cell transplantation as a percentage of the control eye (histogram). Abbreviations: NMDA, N-methyl-D-aspartate; Post-transpl, post-transplantation; Pretranspl, pretransplantation; STR, scotopic threshold response.

resemble the anatomy of the human eye. Therefore, although previous studies have focused on the delivery of stem cell-derived RGCs to the small rodent retina, the present study has evaluated new approaches for the transplantation of Müller-derived RGC onto the retina of a larger mammalian eye.

Our results showed that intravitreal injection of hMGSC-RGCs into the cat eye led to the formation of large aggregates of transplanted cells within the vitreous, suggesting that the vitreous gel may act as a barrier for inner retinal cell transplantation by causing aggregation of the grafted cells and therefore limiting their attachment and migration into the neural retina. This has not been previously observed in the rat eye, in which the eye is occupied by a relatively large lens that serves as a scaffold for transplanted cells to attach onto the retina [11]. Our findings therefore indicate that

results obtained in rodent models may not be replicated in other species with larger eyes, including humans. Furthermore, despite the immunosuppressive and anti-inflammatory regimen used in this study, human cells elicited a severe inflammatory response when transplanted into the feline eye, as judged by the accumulation of lectin B4 positive microglia around the transplanted cells (Fig. 4). It is therefore possible that this xenograft-induced inflammatory response very likely contributed to the lack of RGC-related improvement of the STR response of the ERG.

To overcome these limitations, we examined the outcomes of allogeneic transplantation in the feline eye by isolating Müller glia with stem cell characteristics from the same species. Müller glia cell preparations isolated from the cat eye were maintained in culture for up to 35 passages without changes in their morphology and phenotypic characteristics. Like that previously observed with Müller glia isolated from the adult human eye [5], feline Müller glia expressed not only characteristic Müller glia markers, including CRALBP, vimentin, and glutamine synthetase, but also markers of neural progenitors such as *Notch*, *Hes1*, *Pax6*, and *Sox2*. In addition, protocols used to differentiate hMGSCs into RGCs in vitro also induced differentiation of feline Müller glia into cells expressing markers of RGCs, as judged by the downregulation of *Hes1* and the upregulation of the RGC markers *Brn3b* and *Isl1* as determined by Western blotting (Fig. 2). Although we could not accurately determine the proportion of cells that differentiated into RGCs because of the lack of specific feline antibodies to *Brn3b*, the enhanced immunocytochemical staining observed, accompanied by the Western blotting results, strongly suggests that the Müller cell population isolated from the feline eye constitutes a stem cell population similar to that previously described in the adult human eye [5].

Allogeneic transplantation of a suspension of fMGSC-RGCs onto the inner retina of a vitrectomized and RGC-depleted feline eye showed that despite grafted cells aggregating in remnant vitreous on the inner retinal surface, they cause an improvement of the STR of the ERG as compared with the same eye after NMDA treatment before cell transplantation. This suggests that the transplanted cells may have had a neuroprotective effect on the damaged RGC, which might have been facilitated by their closer proximity to the retina. Functional outcomes following grafting of stem cells onto the neural retina, with the goal of neural cell replacement and/or neuroprotection, are likely to depend on their capacity to attach to the retina and survive for protracted periods post-transplantation. After transplanting the cellular scaffolds, we did not test specifically for cell viability but did not observe any autofluorescence, cell aggregation, fragmented nuclei, or apoptotic bodies, which are indicators of cell death. In addition, cells were seen to extend long processes, which is also suggestive of cell viability.

On the basis of our observations that cell transplantation into the vitreous caused cells to aggregate, we designed a protocol that could facilitate the survival and attachment of transplanted cells onto the retina. For this purpose, we constructed cellular scaffolds using compressed collagen gels [14, 15] that were seeded with enriched populations of fMGSC-RGCs for transplantation onto the retina in vitrectomized eyes. Interestingly, our results showed that the scaffolds facilitated attachment of the grafted cells onto the feline retina, as judged by live OCT imaging, as well as by confocal microscopy examination of immunostained retinal sections ex vivo. Although grafted cells attached onto the retina and extended long processes across the retinal surface, they did not integrate into the RGC layer and did not project axons

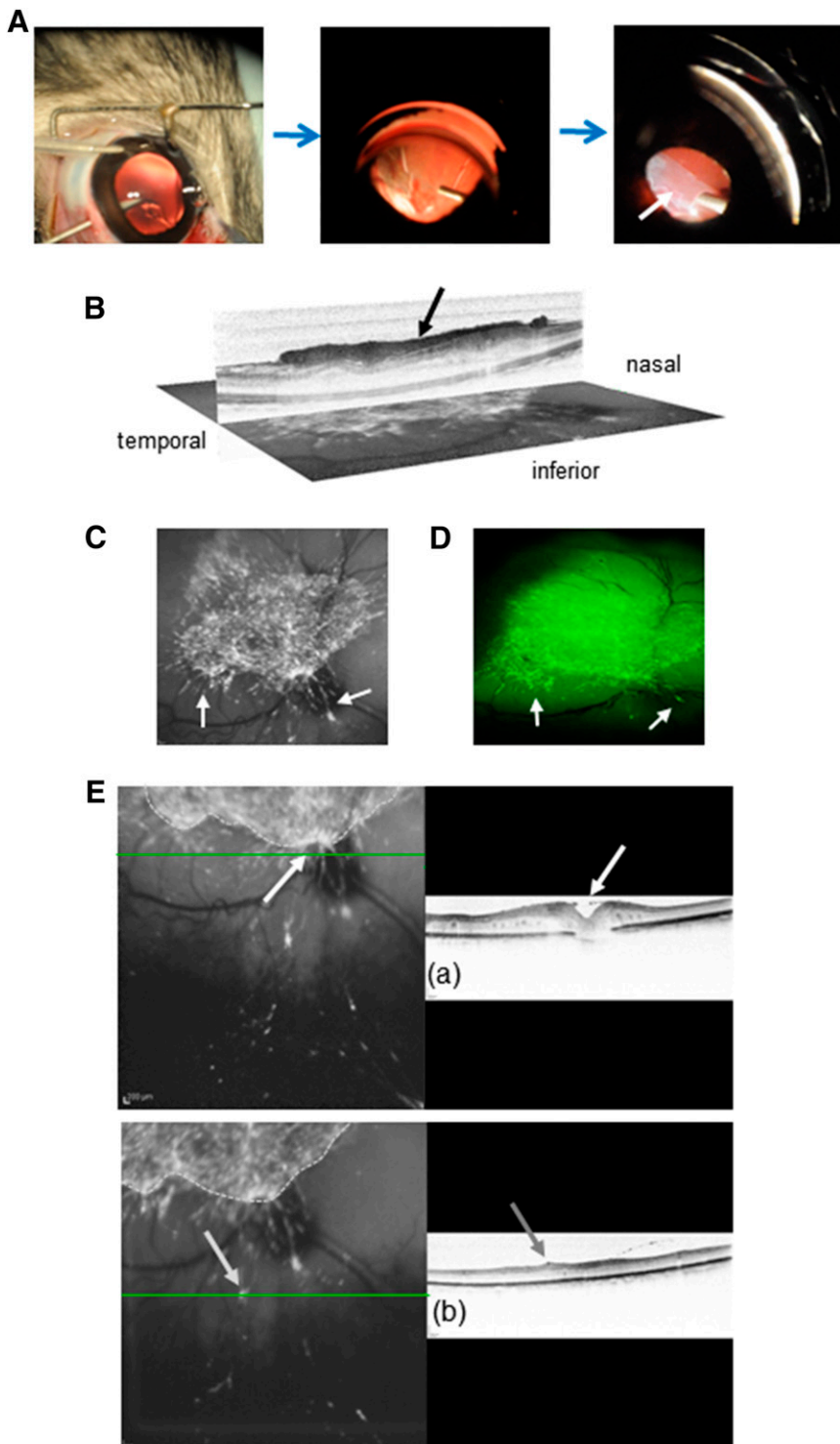


Figure 5. Transplantation of cellular scaffolds. **(A)**: Images illustrating the surgical procedure used for transplantation of cellular scaffolds. From left to right, images illustrate the lensectomy, vitrectomy, and transplantation of cellular scaffolds. Scaffold has the appearance of a white translucent membrane (white arrow). **(B)**: Representative infrared reflectance image and ocular coherence tomography (OCT) scan in a feline retina at 2 weeks after transplantation of a cellular scaffold containing retinal ganglion cells derived from feline Müller glial stem cells (black arrow). The OCT image is overlaid on an en face scan across the fundus that illustrates the site of scaffold attachment. **(C)**: Scanning laser ophthalmoscope image of the same eye fundus showing the cellular scaffold attached to the inner retinal surface of the transplanted eye. Cells can be seen migrating away from the scaffold onto the retinal surface (white arrows). **(D)**: Fluorescent image of the same scaffold viewed under the dissecting microscope showing the same cells migrating away from the scaffold (arrows). **(E)**: Green lines show the positions of the OCT images shown in the reflectance images on the right. Arrows indicate the position of cells migrating at the edge scaffold over the optic nerve head (**Ea**) and at a distance below the optic nerve head (**Eb**).

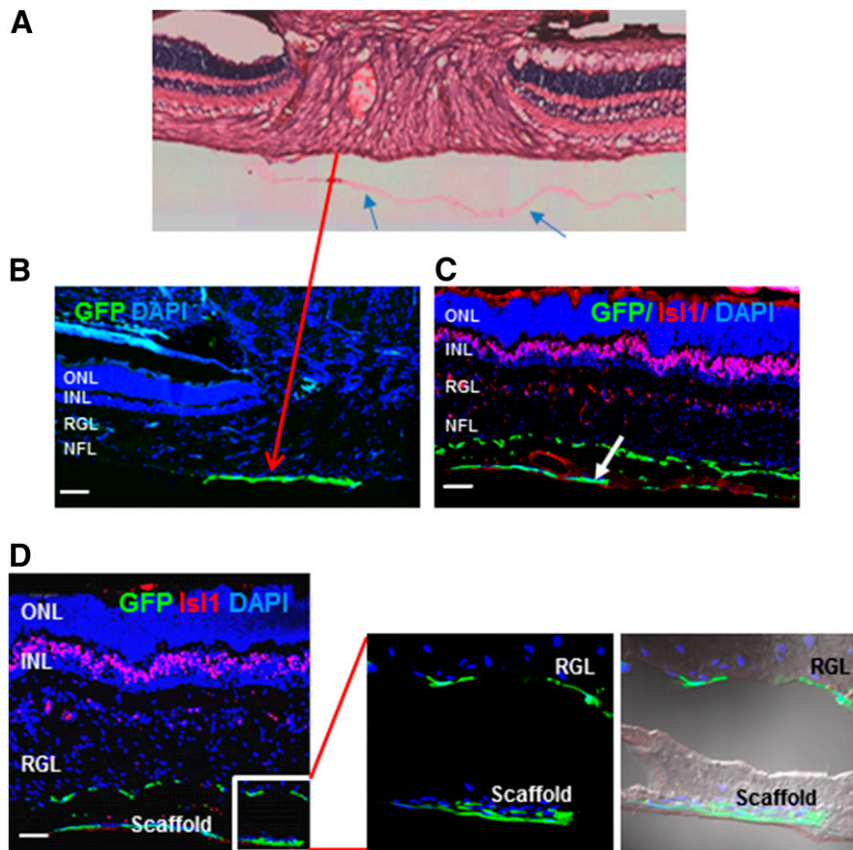


Figure 6. Transplantation of cellular scaffolds containing retinal ganglion cells (RGCs) derived from feline Müller glia with stem cell characteristics (fMGSCs). **(A)**: Histological section of retina transplanted with a cellular scaffold seeded with GFP-labelled fMGSC-RGCs 2 weeks after the procedure. H&E staining shows the collagen scaffold adjacent to the retina and optic nerve head (blue arrows). **(B)**: Confocal microscopic image of a section of the same eye shown in **(A)**, in which the transplanted cells (GFP, green) can be observed attached to the nerve fiber layer without evidence of migration into the optic nerve (red arrow). Scale bar = 100 μ m. **(C)**: Confocal image showing widespread attachment of the transplanted cells (GFP, green) onto the retina at a distance from the optic nerve head without migration into the RGC. Cellular scaffold can be observed detached from the retina (white arrow). Scale bar = 100 μ m. **(D)**: Confocal section of an eye transplanted with a cellular scaffold stained for Isl1 (Alexa 555, red). Scale bar = 100 μ m. The section marked in white is magnified on the right. As observed under Nomarski illumination (far-right image), the scaffold was clearly seen away from the retina, and the area in close proximity to the retinal RGL was devoid of cells, with the cells appearing to have migrated from the scaffold onto the retinal surface. Abbreviations: DAPI, 4',6'-diamino-2-phenylindole; GFP, green fluorescent protein; INL, inner nuclear layer; ONL, outer nuclear layer; RGL, retinal ganglion cell layer.

into the optic nerve, even when scaffolds were placed onto the surface of the optic nerve head itself. Importantly, despite their lack of integration, transplanted cells induced a marked improvement of RGC function as measured by the STR and PhNR of the ERG. Given the larger size of the cat eye in comparison with the rat, one should consider that the nerve fiber layer and inner limiting membrane would also be inhibitory for graft migration and integration. For this reason, and to facilitate these processes, we used ChABC in addition to the vitrectomy. Chondroitinase ABC, used to promote cell migration in this study, could potentially cause improvement of retinal function. Although we did not use chondroitinase alone to restrict the number of animals used, we had undertaken previous studies in the rat, in which we showed that chondroitinase did not have any effects on the retina [35]. However, given the thickness of the nerve fiber layer in the cat, the dose of ChABC used might not have been sufficient to breakdown the inner limiting membrane. This merits further investigations in animal models with a large eye.

It is well documented that functional damage to RGCs in experimental models of glaucoma is due to early disruption of axonal transport and neural synapses and that this occurs before RGCs

undergo apoptosis and irreversible damage [36]. In the present study, we used a model of NMDA-induced excitotoxicity of RGCs, characterized by intracellular accumulation of Ca^{2+} that leads to activation of neurotoxic signaling cascades and consequent damage to the cell membrane, cytoskeleton, and DNA [37]. Although this model does not accurately mimic the pattern of RGC cell death observed in glaucoma, it shows the pathological features of depletion of RGC function observed in this condition, as demonstrated by electroretinography. At present there are no animal models of experimentally induced glaucoma that truly resemble this condition in humans, and despite the existence of spontaneous models of feline glaucoma, the variability in the onset of this condition [38] limits their use for experimental studies. Nevertheless, the present observations that a significant improvement of RGC function was induced by transplantation of fMGSC-RGCs in feline eyes depleted of RGCs suggest that these cells have the potential to improve RGC function, possibly by conferring neuroprotection to remaining and injured RGC cells.

This investigation aimed both to optimize cell delivery techniques onto the inner retina of the large mammalian eye and to examine whether it was possible to mimic the partial recovery

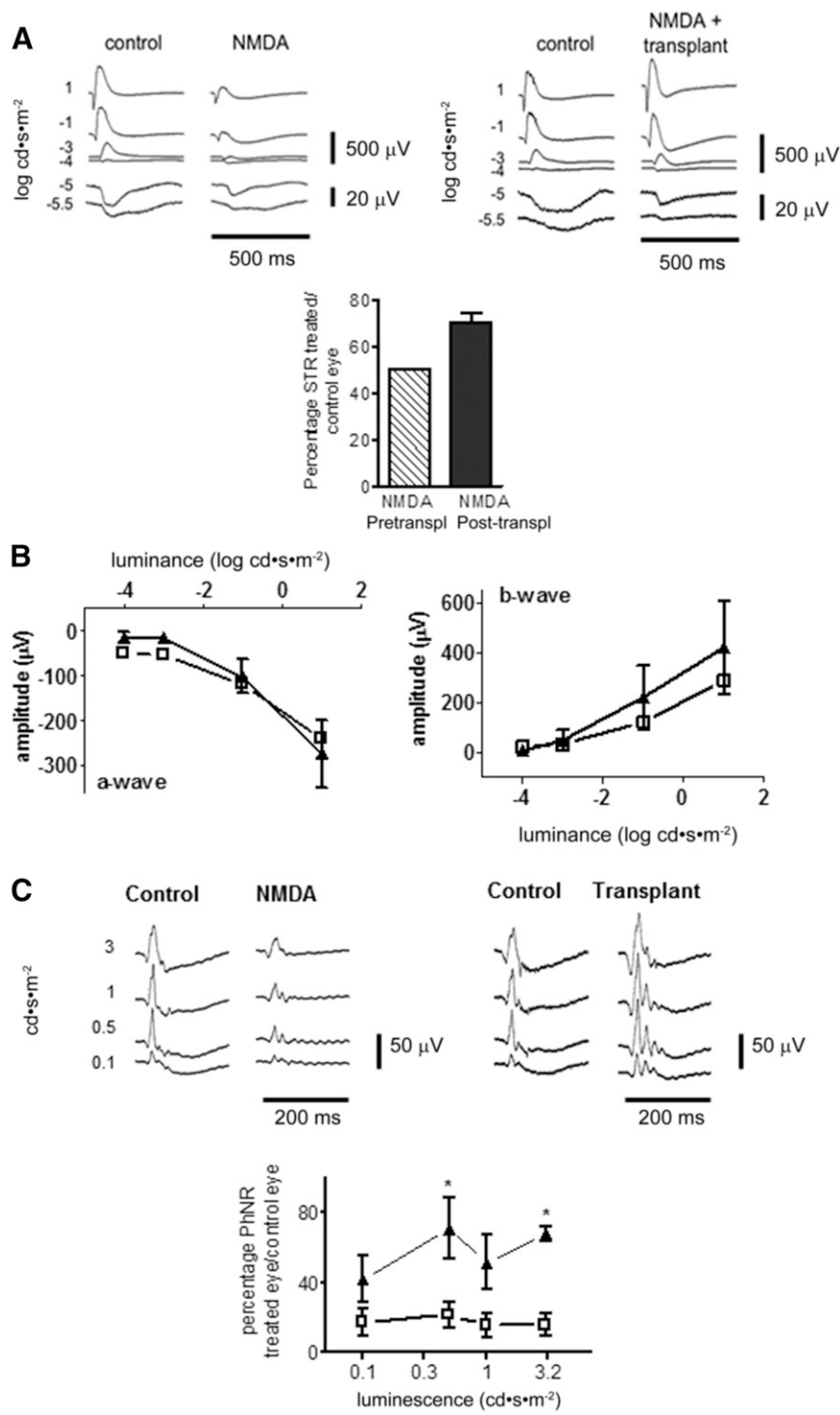


Figure 7. Electrotoretinogram (ERG) response to transplantation of cellular scaffolds containing retinal ganglion cells (RGCs) derived from feline Müller glial stem cells (fMGSCs). **(A)**: Typical recordings depicting the effects of transplantation of scaffolds containing fMGSC-RGCs on the scotopic flash ERG. As shown in the histogram, the amplitude of the STR measured as the percentage of the treated over the control eye was improved after NMDA injection followed by transplantation ($n = 2$) in comparison with intravitreal injection of 1.5 mmol/l NMDA alone (pretransplant). STR is indicated by arrows. **(B)**: The amplitudes of the scotopic a- and b-waves remained unaffected by transplantation of scaffolds containing fMGSC-RGCs (filled triangles) in comparison with control eyes (filled circles) at flash intensities ranging from 10^{-4} to 10^{-1} cd•s•m⁻² ($p > .05$; $n = 3$). **(C)**: Example of traces depicting the effects of transplantation of cellular scaffolds on the PhNR. PhNR is indicated by arrows. The data plotted in the graph show that the PhNR was significantly improved following transplantation of fMGSC-RGCs placed on the scaffolds (filled triangles; *, $p < .05$; $n = 4$) in comparison with intravitreal injection of 1.5 mmol/l NMDA alone (empty squares). Abbreviations: NMDA, N-methyl-D-aspartate; PhNR, photopic negative response; Post-transpl, post-transplantation; Pretranspl, pretransplantation; STR, scotopic threshold response.

of retinal function previously observed in rat models of RGC damage following transplantation of hMGSC-RGCs. In this study, to assess any potential improvement of retinal function by transplantation of RGCs derived from fMGSCs, RGC damage induced by NMDA treatment was intended to cause only partial impairment. We did not see transplanted cells integrating into the RGC layer, and this might be partly ascribed to the short duration of the study. However, the cat is very susceptible to the side effects of immunosuppressant drugs, making it difficult to undertake long-term experiments involving immunosuppression in this species. Despite the lack of integration, we observed improvement of the RGC function, suggesting that this effect is due to a neurotrophic effect of the transplanted cells. It remains unclear whether the partial recovery of function was due to increased RGC survival or axon regeneration induced by neurotrophic factors, but further studies would be needed to clarify these effects. Müller glia has been shown to produce ciliary neurotrophic factor (CNTF) [39], FGF-2, brain-derived neurotrophic factor (BDNF), and glial cell line-derived neurotrophic factor [40], whereas RGCs have been shown to produce factors such as insulin growth factor and neurotrophin 3 [41], as well as BDNF [42]. Our suggestion that the improvement on the RGC function was due to a neurotrophic effect of the transplanted cells is supported by observations by others that BDNF and CNTF decrease RGC loss in animal models of optic nerve damage [43] and that overexpression of BDNF in the retina protects RGCs in a rat model of glaucoma [44]. Furthermore, there is evidence that intravitreal administration of CNTF stimulates axon regeneration of retinal ganglion cells [45]. Given that a combination of differentiated RGC and undifferentiated Müller glia were transplanted, it is possible that neurotrophins were released by both cell types. However, further studies are needed to determine these effects. Compelling evidence for the role of neurotrophins on RGC protection has led to the development of clinical trials using encapsulated human cells genetically modified to produce high levels of CNTF [46].

CONCLUSION

Since Müller glia are capable of producing a variety of neurotrophic factors, from the present observations it can be suggested that the neurotrophic potential of Müller glia with stem cell characteristics should be further explored for the design of alternative

neuroprotective therapies for glaucoma. Furthermore, it can be proposed that promoting cell attachment onto the retina could be of value for sustained inner retinal neuroprotection, and this warrants further investigations.

ACKNOWLEDGMENTS

This work was supported by the Medical Research Council (Grants 90465 and G0900002), the Helen Hamlyn Trust in memory of Paul Hamlyn, Fight for Sight (by a donation from Tony Bickford), Moorfields Special Trustees, the National Institute for Health Research Biomedical Research Centre at Moorfields Eye Hospital and University College London Institute of Ophthalmology and the University College London Institute Therapeutic Innovation Fund supported by the Wellcome Trust, and the National Institute for Health Research at University College London Institute. G.J.M. was supported by National Institutes of Health Career Development Grant K08 EY018609.

AUTHOR CONTRIBUTIONS

S.B.: collection and assembly of data, data analysis and interpretation, manuscript writing, final approval of manuscript; K.E. and H.J.: collection and assembly of data, data analysis and interpretation, final approval of manuscript; M.F.J.: collection and assembly of data, final approval of manuscript; R.A.B.: provision of study material, final approval of manuscript, biomaterial development; G.J.M.: protocol development, final approval of manuscript; D.G.C.: collection of data, final approval of manuscript; P.T.K.: discussions for conception and design, final approval of manuscript; G.A.L.: conception and design, financial support, data analysis and interpretation, manuscript writing, final approval of manuscript.

DISCLOSURE OF POTENTIAL CONFLICTS OF INTEREST

R.A.B. is inventor and holds intellectual property rights (patent held by employer, University College London Institute; licensed to TAP Biosystems Ltd.). P.T.K. is coinventor with G.A.L. University College London holds the patent for Müller cells. G.A.L. and P.T.K. have uncompensated intellectual property rights. The other authors indicated no potential conflicts of interest.

REFERENCES

- 1 Diekmann H, Fischer D. Glaucoma and optic nerve repair. *Cell Tissue Res* 2013;353:327–337.
- 2 Quigley HA. Neuronal death in glaucoma. *Prog Retin Eye Res* 1999;18:39–57.
- 3 Raymond PA, Barthel LK, Bernardos RL et al. Molecular characterization of retinal stem cells and their niches in adult zebrafish. *BMC Dev Biol* 2006;6:36.
- 4 Bhatia B, Singhal S, Lawrence JM et al. Distribution of Müller stem cells within the neural retina: Evidence for the existence of a ciliary margin-like zone in the adult human eye. *Exp Eye Res* 2009;89:373–382.
- 5 Lawrence JM, Singhal S, Bhatia B et al. MIO-M1 cells and similar muller glial cell lines derived from adult human retina exhibit neural stem cell characteristics. *STEM CELLS* 2007;25:2033–2043.
- 6 Singhal S, Bhatia B, Jayaram H et al. Human Müller glia with stem cell characteristics differentiate into retinal ganglion cell (RGC) precursors in vitro and partially restore RGC function in vivo following transplantation. *STEM CELLS TRANSLATIONAL MEDICINE* 2012;1:188–199.
- 7 Bull ND, Limb GA, Martin KR. Human Müller stem cell (MIO-M1) transplantation in a rat model of glaucoma: Survival, differentiation, and integration. *Invest Ophthalmol Vis Sci* 2008;49:3449–3456.
- 8 Becker S, Jayaram H, Limb GA. Recent advances towards the clinical application of stem cells for retinal regeneration. *Cells* 2012;1:851–873.
- 9 Sieving PA, Frishman LJ, Steinberg RH. Scotopic threshold response of proximal retina in cat. *J Neurophysiol* 1986;56:1049–1061.
- 10 Saszik SM, Robson JG, Frishman LJ. The scotopic threshold response of the dark-adapted electroretinogram of the mouse. *J Physiol* 2002;543:899–916.
- 11 Jayaram H, Becker S, Eastlake K et al. Optimized feline vitrectomy technique for therapeutic stem cell delivery to the inner retina. *Vet Ophthalmol* 2014;17:300–304.
- 12 Narfström K, Deckman KH, Menotti-Raymond M. Cats: A gold mine for ophthalmology. *Annu Rev Anim Biosci* 2013;1:157–177.
- 13 Limb GA, Salt TE, Munro PM et al. In vitro characterization of a spontaneously immortalized human Muller cell line (MIO-M1). 2002;43:864–869.
- 14 Brown RA, Wiseman M, Chuo C-B et al. Ultrarapid engineering of biomimetic materials and tissues: Fabrication of nano- and microstructures by plastic compression. *Adv Funct Mater* 2005;15:1762–1770.
- 15 Levis HJ, Brown RA, Daniels JT. Plastic compressed collagen as a biomimetic substrate for human limbal epithelial cell culture. *Biomaterials* 2010;31:7726–7737.

- 16** Siliprandi R, Canella R, Carmignoto G et al. *N*-Methyl-D-aspartate-induced neurotoxicity in the adult rat retina. *Vis Neurosci* 1992; 8:567–573.
- 17** Singhal S, Lawrence JM, Salt TE et al. Triamcinolone attenuates macrophage/microglia accumulation associated with NMDA-induced RGC death and facilitates survival of Müller stem cell grafts. *Exp Eye Res* 2010;90:308–315.
- 18** Kwong JM, Lam TT. *N*-Methyl-D-aspartate (NMDA) induced apoptosis in adult rabbit retinas. *Exp Eye Res* 2000;71:437–444.
- 19** Nakazawa T, Watanabe M, Kudo H et al. Susceptibility to *N*-methyl-D-aspartate toxicity in morphological and functional types of cat retinal ganglion cells. *Jpn J Ophthalmol* 2010;54:156–162.
- 20** Bui BV, Edmunds B, Cioffi GA et al. The gradient of retinal functional changes during acute intraocular pressure elevation. *Invest Ophthalmol Vis Sci* 2005;46:202–213.
- 21** Wakili N, Horn FK, Jünemann AG et al. The photopic negative response of the blue-on-yellow flash-electroretinogram in glaucomas and normal subjects. *Doc Ophthalmol* 2008;117:147–154.
- 22** Rangaswamy NV, Shirato S, Kaneko M et al. Effects of spectral characteristics of ganzfeld stimuli on the photopic negative response (PhNR) of the ERG. *Invest Ophthalmol Vis Sci* 2007;48:4818–4828.
- 23** Yamashita H, Yamada-Nakayama C, Sugihara K et al. Functional and morphological effects of β -estradiol in eyes with *N*-methyl-D-aspartate-induced retinal neurotoxicity in rats. *Exp Eye Res* 2011;93:75–81.
- 24** Inokuchi Y, Shimazawa M, Nakajima Y et al. A $\text{Na}^+/\text{Ca}^{2+}$ exchanger isoform, NCX1, is involved in retinal cell death after *N*-methyl-D-aspartate injection and ischemia-reperfusion. *J Neurosci Res* 2009;87:906–917.
- 25** Bouhenni RA, Dunmire J, Sewell A et al. Animal models of glaucoma. *J Biomed Biotechnol* 2012;2012:692609.
- 26** Niemeyer G. ERG components of negative polarity from the inner retina and the optic nerve response. *Doc Ophthalmol* 2005;111:179–189.
- 27** Fortune B, Bui BV, Morrison JC et al. Selective ganglion cell functional loss in rats with experimental glaucoma. *Invest Ophthalmol Vis Sci* 2004;45:1854–1862.
- 28** Holcombe DJ, Lengefeld N, Gole GA et al. Selective inner retinal dysfunction precedes ganglion cell loss in a mouse glaucoma model. *Br J Ophthalmol* 2008;92:683–688.
- 29** Viswanathan S, Frishman LJ, Robson JG et al. The photopic negative response of the macaque electroretinogram: Reduction by experimental glaucoma. *Invest Ophthalmol Vis Sci* 1999;40:1124–1136.
- 30** Dahlmann-Noor A, Vijay S, Jayaram H et al. Current approaches and future prospects for stem cell rescue and regeneration of the retina and optic nerve. *Can J Ophthalmol* 2010;45: 333–341.
- 31** Dahlmann-Noor AH, Vijay S, Limb GA et al. Strategies for optic nerve rescue and regeneration in glaucoma and other optic neuropathies. *Drug Discov Today* 2010;15:287–299.
- 32** Cho JH, Mao CA, Klein WH. Adult mice transplanted with embryonic retinal progenitor cells: New approach for repairing damaged optic nerves. *Mol Vis* 2012;18:2658–2672.
- 33** Hambright D, Park KY, Brooks M et al. Long-term survival and differentiation of retinal neurons derived from human embryonic stem cell lines in un-immunosuppressed mouse retina. *Mol Vis* 2012;18:920–936.
- 34** Becker S, Singhal S, Jones MF et al. Acquisition of RGC phenotype in human Müller glia with stem cell characteristics is accompanied by upregulation of functional nicotinic acetylcholine receptors. *Mol Vis* 2013; 19:1925–1936.
- 35** Singhal S, Lawrence JM, Bhatia B et al. Chondroitin sulfate proteoglycans and microglia prevent migration and integration of grafted Müller stem cells into degenerating retina. *STEM CELLS* 2008;26:1074–1082.
- 36** Frankfort BJ, Khan AK, Tse DY et al. Elevated intraocular pressure causes inner retinal dysfunction before cell loss in a mouse model of experimental glaucoma. *Invest Ophthalmol Vis Sci* 2013;54:762–770.
- 37** Sattler R, Tymianski M. Molecular mechanisms of glutamate receptor-mediated excitotoxic neuronal cell death. *Mol Neurobiol* 2001; 24:107–129.
- 38** McLellan GJ, Miller PE. Feline glaucoma: A comprehensive review. *Vet Ophthalmol* 2011; 14(suppl 1):15–29.
- 39** Ju WK, Lee MY, Hofmann HD et al. Expression of CNTF in Müller cells of the rat retina after pressure-induced ischemia. *Neuroreport* 1999; 10:419–422.
- 40** Harada C, Harada T, Quah HM et al. Potential role of glial cell line-derived neurotrophic factor receptors in Müller glial cells during light-induced retinal degeneration. *Neuroscience* 2003;122:229–235.
- 41** Martínez-Moreno C, Andres A, Giterman D et al. Growth hormone and retinal ganglion cell function: QNR/D cells as an experimental model. *Gen Comp Endocrinol* 2014;195:183–189.
- 42** Vecino E, García-Crespo D, García M et al. Rat retinal ganglion cells co-express brain-derived neurotrophic factor (BDNF) and its receptor TrkB. *Vision Res* 2002;42:151–157.
- 43** Wang Y, Brown DP Jr., Duan Y et al. A novel rodent model of posterior ischemic optic neuropathy. *JAMA Ophthalmol* 2013;131: 194–204.
- 44** Martin KR, Quigley HA, Zack DJ et al. Gene therapy with brain-derived neurotrophic factor as a protection: Retinal ganglion cells in a rat glaucoma model. *Invest Ophthalmol Vis Sci* 2003;44:4357–4365.
- 45** Müller A, Hauk TG, Leibinger M et al. Exogenous CNTF stimulates axon regeneration of retinal ganglion cells partially via endogenous CNTF. *Mol Cell Neurosci* 2009;41:233–246.
- 46** NT-501 CNTF implant for glaucoma: Safety, neuroprotection and neuroenhancement. ClinicalTrials.gov identifier: NCT01408472. Available at <https://clinicaltrials.gov/ct2/show/NCT01408472?term=NCT01408472&rank=1>. Accessed September 13, 2015.



See www.StemCellsTM.com for supporting information available online.